Current updates of the water-vapor line list in *HITRAN*: A new "Diet" for air-broadened half-widths

Iouli E. Gordon[a], Laurence S. Rothman[a,*], Robert R. Gamache[b], David Jacquemart[c], Chris Boone[d], Peter F. Bernath[d,e], Mark W. Shephard[f], Jennifer S. Delamere[f], Shepard A. Clough[f]

[a]*Harvard-Smithsonian Center for Astrophysics, Atomic and Molecular Physics Division, Cambridge, MA 02138-1516, USA*
[b]*University of Mass. Lowell, Department of Environmental, Earth & Atmospheric Sciences, Lowell, MA 01854, USA*
[c]*Université Pierre et Marie Curie-Paris 6, Laboratoire de Dynamique, Interactions et Réactivité, CNRS, Paris Cedex 05, France*
[d]*University of Waterloo, Department of Chemistry, Waterloo, Ontario, Canada N2L 3G1*
[e]*University of York, Department of Chemistry, Heslington, York YO10 5DD, UK*
[f]*Atmospheric and Environmental Research (AER), Inc., Lexington, MA 02421, USA*

Abstract

The current edition of the *HITRAN* compilation employed a sophisticated algorithm for combining measurements available for the air-broadened half-widths of water-vapor absorption lines with theoretical values. Nevertheless, some of the values in the *HITRAN* database were found to be far from ideal, due to large dispersions that still exist in the experimental or theoretical methods. Therefore, new criteria were developed for introducing the best available air-broadened half-widths into *HITRAN*, based on physical principles and statistics. This update concerns the three most abundant isotopologues of water, with the values for $H_2^{17}O$ and $H_2^{18}O$ being the ones from analogous transitions of the principal isotopologues. The new parameters have been tested in different remote-sensing applications and improved constituent profiles were obtained. In total, air-broadened half-width values were updated for 11,787 transitions of water vapor in the *HITRAN* database (6789 for $H_2^{16}O$, 2906 for $H_2^{17}O$, and 2092 for $H_2^{18}O$). Some additional updates to the water-vapor line list are also presented. The resultant file (01_hit06.par) was uploaded to the *HITRAN* website (http://www.cfa.harvard.edu/hitran/) in September 2006.
© 2007 Elsevier Ltd. All rights reserved.

1. Introduction

The line-by-line portion of the *HITRAN* database [1] consists of high-resolution spectroscopic parameters for 39 molecules of atmospheric interest, including many of their isotopologs. For every transition, *HITRAN* provides the vacuum line position, the line intensity, the Einstein *A*-coefficient and statistical weights, the air-broadened half-width (γ_{air}), the self-broadened half-width, the lower state energy, the temperature-dependence

*Corresponding author. Tel.: +1 617 495 7474; fax: +1 617 496 7519.
E-mail address: lrothman@cfa.harvard.edu (L.S. Rothman).

exponent of γ_{air}, the air pressure-induced line shift, and lower and upper state vibrational and rotational quantum numbers.

The data for water vapor are very important for atmospheric sciences. Water vapor is the principal absorber of longwave radiation in the terrestrial atmosphere and it has a profound effect on the atmospheric energy budget in many spectral regions. The *HITRAN* database lists more than 64,000 significant transitions of water vapor ranging from the microwave region to the visible, with intensities that cover many orders of magnitude. These transitions are used, or have to be accounted for, in various remote-sensing applications.

Out of all water-vapor spectroscopic parameters in *HITRAN*, the intensity of weak lines and the overall pressure-broadening coefficients are the largest sources for uncertainty in remote-sensing retrievals [2]. For H_2O, the half-width parameters have the largest dynamic range of any molecule contained in *HITRAN* and they contribute on a par with the intensities to the radiance and transmission simulations in regimes of tropospheric pressure, i.e. where collision-broadening by air is significant. For accurate retrievals that are achievable with the high signal-to-noise and wide spectral coverage of current satellite-borne experiments, it is required to know the half-width and its temperature dependence better than a 3% uncertainty for strong lines and 10% for weak lines [3]. For the current compilation [1] (hereafter referred to as *HITRAN*2004), a great effort had been made to provide the most accurate value of the air-broadened half-width, γ_{air}, for every transition of the $H_2^{16}O$, $H_2^{18}O$, and $H_2^{17}O$ isotopologues of water. The algorithm used data from several theoretical, experimental, and semi-empirical datasets. The hierarchy of the sources from which γ_{air} was determined is described below.

1.1. The database of experimental measurements

The database of experimental measurements of collision-induced parameters was created by Gamache and Hartmann (hereafter referred to as GH database) [3]. It lists the vast majority of the experimental data from different sources, reported prior to the publication of Ref. [3]. The dataset spans the region 0–22,640 cm^{-1}, listing values for γ_{air} (with reported experimental uncertainties) from over 40 sources. The γ_{air} values for over 3000 transitions have been measured more than once and those for over 6000 transitions have been measured only once. Overall there are more than 14,000 entries in the GH database.

1.2. Smoothed values

A database of smoothed values for collision-induced parameters has been created by Toth and is available on his website (http://mark4sun.jpl.nasa.gov/data/spec/H2O). The smoothing procedure is explained in detail in Refs. [4,5]. The transitions from 600 to 8000 cm^{-1} measured in Refs. [4,5] were grouped into subsets with $v_2' = 0$ and $v_2' > 0$ and then least-squares fitted to the empirical function (Eq. (4) in Ref. [5]) in terms of "families" of rotational transitions.

1.3. The database of values calculated using the complex Robert–Bonamy method

The complex Robert–Bonamy (CRB) method [6] was applied in Refs. [7,8] to calculate air-broadened half-widths of water vapor. A compilation of these calculations is available at http://faculty.uml.edu/Robert_Gamache. The calculations are obtained for 6040 transitions that involve states with $J \leqslant 18$ in the 0–3810 cm^{-1} region. The details of the calculations are given in the aforementioned references. The CRB values in general agree well with experiments [7,8], except for some high-J transitions where the comparison is not always informative since such transitions are usually weak in experimental spectra and hence accurate experimental data are limited. In turn, the CRB calculations are not expected to be as accurate at high J's due to the higher uncertainty in the wavefunctions and energies obtained from diagonalizing the Watson Hamiltonian [9]. While the experimental γ_{air} for transitions with $|\Delta K| > 1$ are also limited or lack accuracy due to the relatively low intensity of such transitions, one should expect the accuracy of CRB values not to suffer since the information needed for the calculations is that of the states and is not dependent on the ΔK of the transition.

1.4. Database of semi-empirical values

In the semi-empirical treatment of Jacquemart et al. [10], experimental data from Refs. [11–15] and theoretical (CRB) data from Refs. [7,16,17] for each transition were taken and then separated into subsets of the data for transitions that would involve the same lower and upper state rotational quantum numbers, but where the vibrational quantum numbers were not necessarily the same. These data were then fit to the equation that describes the vibrational dependence of γ_{air} [15]:

$$\gamma[(v'_1, v'_2, v'_3)f \leftarrow (v''_1, v''_2, v''_3)i] = \gamma^0_{f \leftarrow i} + A_{f \leftarrow i}(0.3\Delta v_1 + 0.7\Delta v_2 + 0.3\Delta v_3)^2, \tag{1}$$

where v_i represents the quantum numbers associated with the normal mode of vibration i. The prime and double prime are used, respectively, for the upper and lower levels of the transition, and Δv_i is equal to $v'_i - v''_i$. For water vapor, the notations i and f correspond, respectively, to the rotational quantum numbers (J'', K''_a, K''_c) and (J', K'_a, K'_c). $\gamma^0_{f \leftarrow i}$ is equivalent to the half-width for a pure rotational transition which corresponds to $(v'_1 = 0, v'_2 = 0, v'_3 = 0)f \leftarrow (v''_1 = 0, v''_2 = 0, v''_3 = 0)j$. The coefficients $\gamma^0_{f \leftarrow i}$ and $A_{f \leftarrow i}$ deduced from the fit allow one to obtain any air-broadening coefficient of transitions having the same rotational quantum numbers but different vibrational quantum numbers. Obvious outliers were eliminated from the fit.

The algorithm used for compiling the air-broadened half-width data in *HITRAN*2004 would first search the GH database: if γ_{air} for the transition was measured more than once the average of all experimentally determined values was taken, if it was measured just once the measurement was taken. It is worth noting that the data from Refs [13,15,18] were not included into the algorithm if they differed from the corresponding values in the semi-empirical database [10] by more than 20%. If the γ_{air} value for a given rotational–vibrational transition did not exist in the GH database, the algorithm then searched the smoothed-values database. If the transition was still not found, the search was extended to the database of CRB values. Finally, if a value for a particular transition was not found in any of the aforementioned databases, the γ_{air} value was derived using the semi-empirical approach of Jacquemart et al. [10]. For the transitions of $H_2^{17}O$ and $H_2^{18}O$ isotopologues, the values from corresponding transitions of $H_2^{16}O$ were adapted if there were no direct measurements.

Overall, the above algorithm has provided a complete set of air-broadened half-widths for all assigned lines in *HITRAN*2004. The unassigned lines were given a default value of $0.07\,cm^{-1}\,atm^{-1}$. Nevertheless, the values of the air-broadened half-width in *HITRAN*2004 were found to be far from ideal when applied to some atmospheric transmission experiments [19,20] (see Section 3 for details). The reason that the sophisticated algorithm for adding air-broadened half-widths of water-vapor transitions into the *HITRAN*2004 database does not always yield an optimum value is simply due to large dispersions in the experimental or theoretical methods that still exist. The experimental spectra are sometimes hard to interpret due to many reasons such as line overlaps, impurities in the cell, etc. The CRB calculations, despite being quite accurate in most of the cases, are still far from perfect due to the different approximations. Both theory and experiment are not accurate when dealing with weak lines with high-J values. The semi-empirical calculations [10] are inheriting the problems of the experimental and theoretical sources even though obvious outliers were eliminated in the course of that work.

In this paper, we will describe the problems arising from using the *HITRAN*2004 list in retrievals of the constituent profiles, the sources of the problems, and a new algorithm that yields a better dataset. The new dataset was validated in different remote-sensing missions. Other updates to the *HITRAN*2004 water-vapor file will be discussed as well. In general, this manuscript explains the new parameters in the 01_hit06.par file that were uploaded to the HITRAN website in September 2006.

2. An improved algorithm

In order to improve the γ_{air} values of water vapor, it was decided to create a hierarchical scheme that would favor one source over another based not on the general quality of the source but on its quality as applied to a particular transition or "family" of transitions. This approach is widely applied by pediatricians in order to control a patient's weight. Every patient has a "normal weight" that can be achieved by losing or gaining

weight, but the recommended diet for every person is different as everyone has a different metabolism, daily activities, etc. We therefore called our new algorithm for adding air-broadened half-widths of water-vapor lines to the *HITRAN* database a "Diet". In this section, the development of the Diet will be discussed and the steps of the algorithm will be summarized.

The GH database [3] aggregates the results of all experimental works that were performed before 2004, including ones dating back to the 1930s. It would be naive to assume that the quality of all experiments and their interpretation was ideal, and, as a first step, it was decided to find and omit the sources that provided consistently inaccurate values.

Fig. 1 shows the ratios of experimental γ_{air} values reported in different sources [4,12,21–30] in the 1000–2000 cm^{-1} region (as an example) to corresponding values calculated by the CRB method plotted against the values of CRB γ_{air}. The values from a certain source are shown only if there were at least five measurements in the selected wavenumber range. While at low values of γ_{air} (effectively, transitions with high *J*) the ratios are not expected to be necessarily very close to 1 since both experiments and theoretical calculations lack accuracy there, at higher values of γ_{air} the ratios are expected to be close to 1. One can see that data from larger datasets such as Zou and Varanasi [12] and Toth [4] agree well with CRB calculations (with rare exceptions), while those from some other references such as Refs. [21,22] often deviate. We have also examined the plots created by Gamache and Hartmann when their database was assembled [3]. Fig. 2 is an example of such an investigation. In Fig. 2 one can see air-broadened half-widths measured for four transitions by three or four independent laboratories, namely the works of Toth [4], Zou and Varanasi [12], Chang and Shaw [21], and Nicolaisen [24]. The error bars represent experimental uncertainties reported in these works. The dashed line is the average half-width that was put into the *HITRAN* 2004 database for these transitions. The numbers AD and Max in the boxes are the average percent differences between any two measurements and the maximum percent difference between any two measurements. It is worth noting that difference is stated in percents of one of the values rather than of the average (as is more common in these types of comparisons). In all four plots (and through most of the dataset), the measurements performed by Chang and Shaw [21] disagree with those of Zou and Varanasi [12] and Toth [4], which are very consistent in general.

It is also clear from Figs. 2 and 3 that it is difficult to correctly estimate experimental uncertainties, as often error bars of different measurements do not overlap.
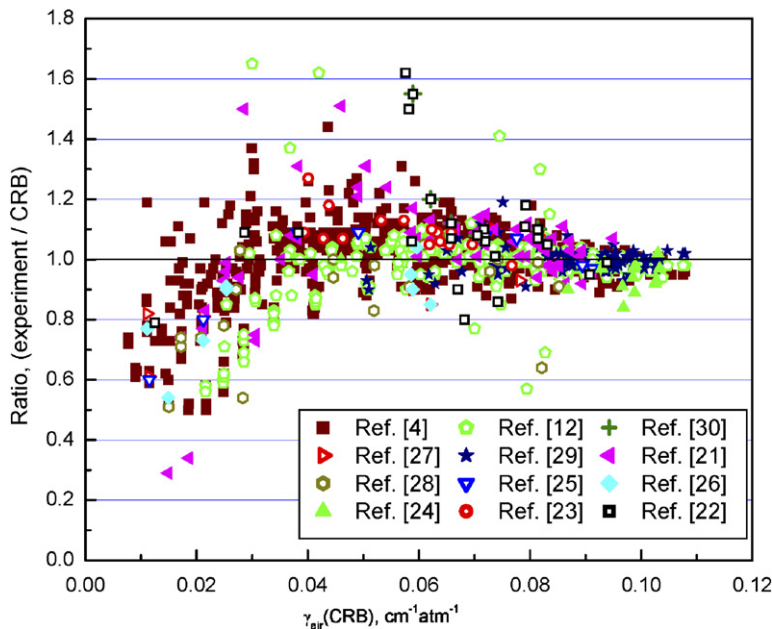

Fig. 1. The ratios of experimental γ_{air} to the corresponding CRB γ_{air} plotted against CRB γ_{air}.
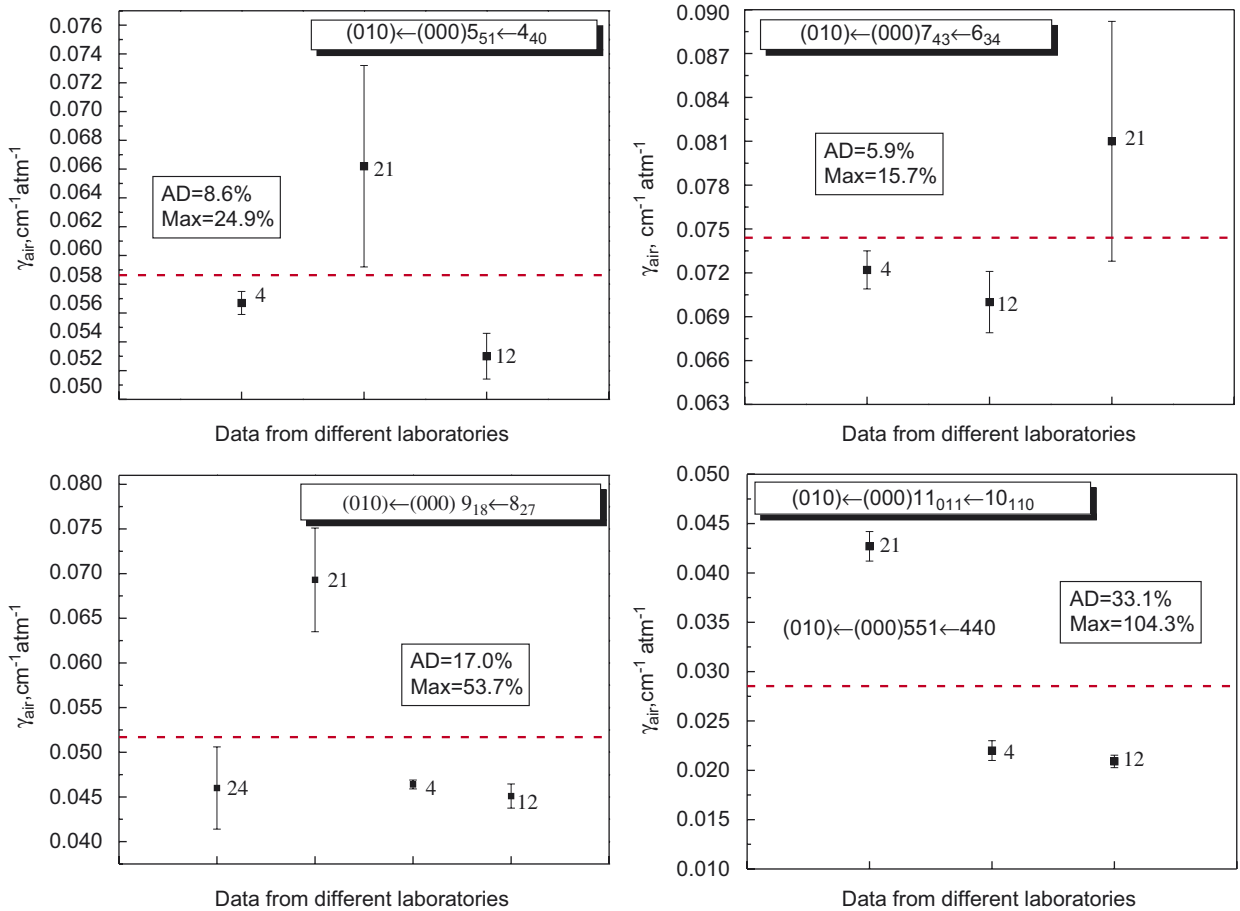
Fig. 2. An example of consistent disagreement of one source of experimental values with others. Upper and lower states involved in the transitions are given in the shadowed boxes as $(v'_1\ v'_2\ v'_3) \leftarrow (v''_1\ v''_2\ v''_3)$, $J'_{K_{a'}K_{c'}} \leftarrow J''_{K_{a''}K_{c''}}$. See text for other details.

After examination of the quality of data from different sources, the data from Refs. [21,22,28,31–35] were omitted from the GH database. The lower quality of some of the data in these sources is corroborated by Toth in Table 5 of Ref. [5]. After a final list was created, it was realized that Ref. [32] in general contains very good data, but the values from this work had not undergone a proper units conversion when incorporated into the GH database and were therefore making a bad contribution to the average. Nevertheless, there are plenty of other accurate measurements existing for the transitions studied in Ref. [32] and the quality of the final half-widths that were incorporated into the new *HITRAN* list had not suffered by omission of these measurements. The values from Ref. [32] are not included in Fig. 1. It should be stated that not all of the measurements in the above references are necessarily inaccurate.

Sometimes, however, it was hard to determine whether one or another experimental work was reliable, since it produced an equal amount of good- and bad-quality data. In Fig. 3a the measurement from Brown et al. [14] agrees better with that from Schermaul et al. [18] than with the one from Merienne et al. [13], whereas in Fig. 3b the measurement from Ref. [14] agrees better with that from Ref. [13] than with the one from Ref. [18]. This is a very common situation observed when scrutinizing the plots. To solve this problem, it was decided to compare the values in the GH database with those from semi-empirical calculations of Jacquemart et al. [10]. If the value in the GH database was more than 20% different from the semi-empirical value for the same transition, it was omitted from the Diet. The quality of the semi-empirical value is strongly dependent on the level of approximation used in the calculations in Ref. [10] (see Ref. [10] for details) and is also affected by the amount and quality of the input data. Nevertheless, it is considered to be within 20% of the real value of γ_{air}
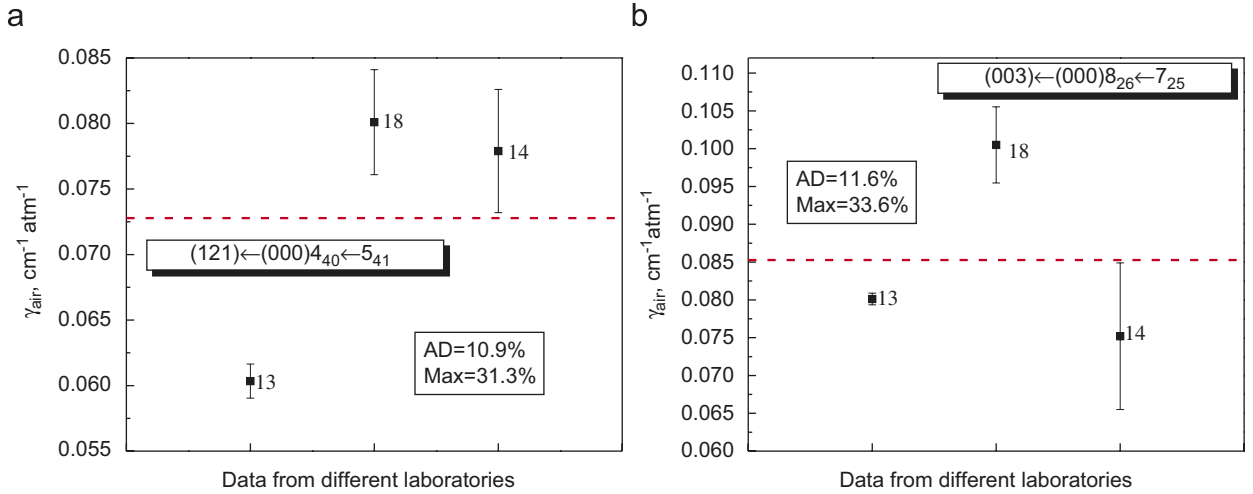
Fig. 3. Illustration of the difficulty of determining which source is more reliable. Upper and lower states involved in the transitions are given in the shadowed boxes as $(v'_1\ v'_2\ v'_3) \leftarrow (v''_1\ v''_2\ v''_3)$, $J'_{Ka'Kc'} \leftarrow J''_{Ka''Kc''}$. See text for details.

Table 1
Definition of U depending on the number of measurements in the GH database

N	Definition of U
$N > 2$	U is an absolute percent difference between the average value and the measurement that deviates the most from it.
$N = 2$	U is a percent difference between measured values with respect to the smaller value out of the two measurements.
$N = 1$	U is a reported experimental uncertainty.

for most of the transitions. We also recommend the use of the semi-empirical dataset when one conducts new experiments, i.e. the new measurements should be expected to be close to the semi-empirical values and if they are not, a careful reanalysis of the particular measurement is in order.

However, 20% accuracy is not satisfactory and further treatment of data is required. The criterion of the data quality was an uncertainty (U), which is defined differently depending on the number of measurements available for a particular transition. The definitions are given in Table 1.

The Diet starts with searching the GH database and it takes an experimental value (or average of experimental measurements if more than one exists) if the following requirements are satisfied:

  (i) for $J_{ave} \leqslant 8$, $U < 7\%$,
 (ii) for $8 < J_{ave} \leqslant 13$, $U < 10\%$,
(iii) for $J_{ave} > 13$, $U < 15\%$,

where $J_{ave} = (J' + J'')/2$.

If the above conditions do not hold, then the experimental average is disregarded and the CRB value is used. If the theoretical value does not exist for this transition, or at $J > 8$ either the upper or the lower state is near the prolate limit defined by $(K_a/J) > 0.75$, the semi-empirical value is used.

The J-dependence of the above constraints on uncertainty is necessary due to the fact that the air-broadened half-widths are getting narrower with increase of J while experimental limitations are the same. Therefore, the uncertainty U (in %) is increasing with J as well, assuming the same quality, although the experimental values may be lacking quality at higher J values, as corresponding transitions are generally weak. Likewise, the quality of the CRB calculations decreases with the increase of J as well. Several constraint limits (both on J's and uncertainties) were tested and it seems that the limits above yield the best result.

For the case when transitions were measured three or more times, it may seem questionable why all measurements are disregarded if the requirements above are not satisfied, instead of eliminating only the measurements that are farthest from the average. The reason is that unfortunately in some cases the outlying measurement may actually be more accurate than the other measurements of the same transition despite their
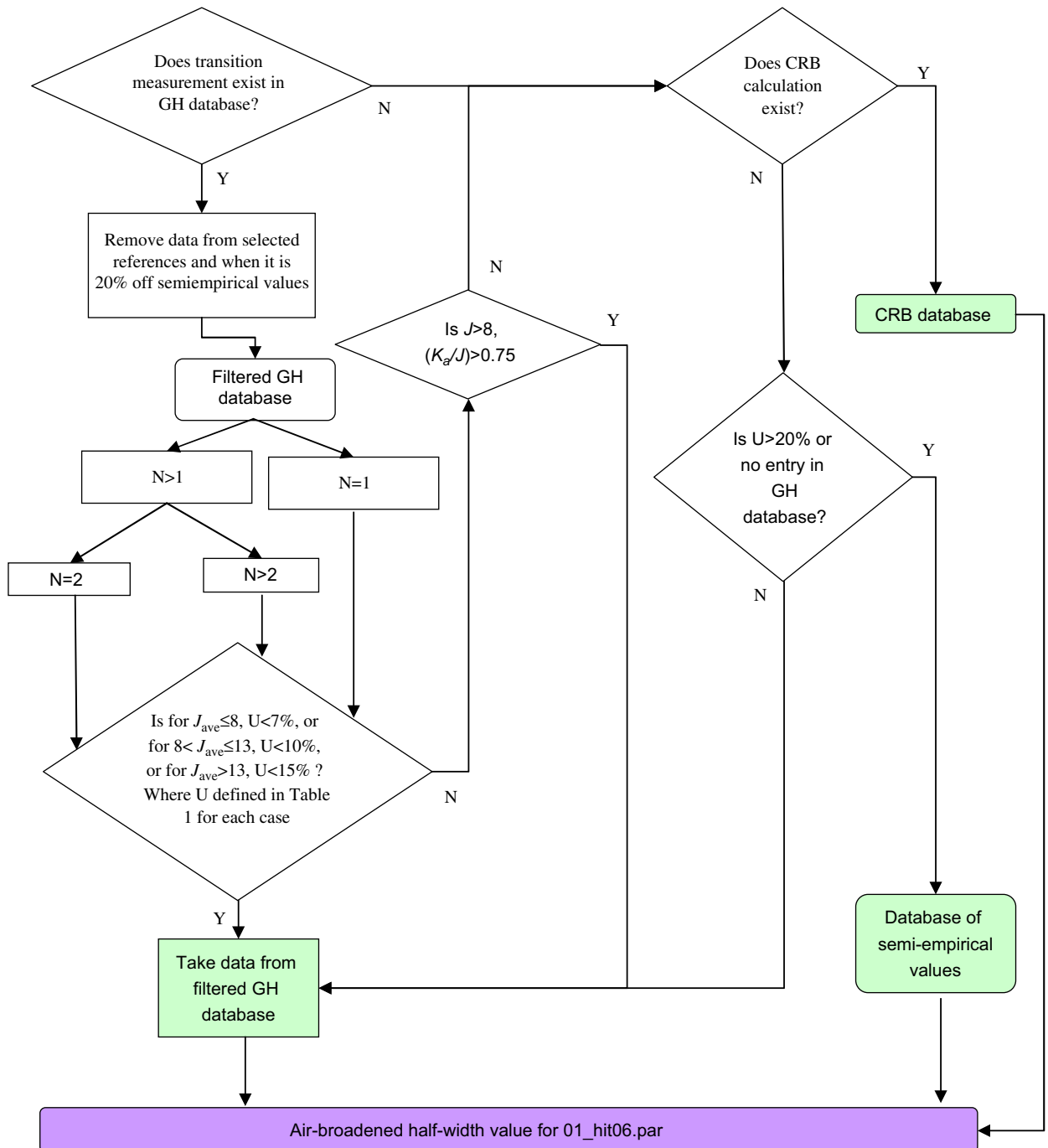

Fig. 4. A flow diagram of the new algorithm for choosing air-broadened half-widths from different sources. N is the number of measurements of air-broadened half-width for a transition.

agreement between each other. Besides, in most of the cases, three or more measurements are only available for moderate J values for which CRB calculations are expected to be accurate within 5%.

The Diet is summarized in the flow diagram given in Fig. 4. Fig. 5 shows the percent differences in the principal isotopologue γ_{air} values of the *HITRAN*2004 database and result of the current work (01_hit06.par file available on the *HITRAN* website). The transitions for which γ_{air} was unchanged as well as the lines that have changed by more than 120% are not shown, and different symbols are used for transitions with different ΔK to give the reader an idea of the relative intensities of the plotted transitions. Below 8000 cm^{-1} one can see a large amount of significant differences, while above that wavenumber the difference does not exceed 20% (with the exception of three transitions around 12,000 cm^{-1}), which is not surprising since in *HITRAN*2004 the data from Refs. [13,15,18] were already tested against the semi-empirical calculations, for 20% agreement. For the three outlying transitions, γ_{air} values in *HITRAN*2004 were originating from the experimental work of Lucchesini et al. [36] and apparently these values were significantly different from semi-empirical predictions. The listing of all transitions for which widths have been changed can be found in the supplementary file.

Although the above algorithm proves to be very efficient, one should not expect the accuracy of the γ_{air} values to be better than 5% (although in many cases they are). Therefore, if better accuracy is needed and potentially achievable, one has to determine the best value manually for a particular case. For example, for the important microwave transition at 22 GHz the Diet chooses the value of 0.0942 cm^{-1} atm^{-1}, which is an average of three experimental measurements (0.0918 cm^{-1} atm^{-1} [37], 0.0965 cm^{-1} atm^{-1} [38], and 0.0942 cm^{-1} atm^{-1} [39]) that have cleared the filtering criteria because they were relatively close to each other, whereas the value from CRB calculations is 0.0920 cm^{-1} atm^{-1} and the value from the corresponding rotational transition in the ν_2 band is 0.0909 cm^{-1} atm^{-1} (current update). This suggests that the current value in the update is overestimated. For the future *HITRAN* edition, we will adapt the value from the newest CRB calculations (0.0918 cm^{-1} atm^{-1}) that include the explicit determination of the velocity integral. Similarly, the new CRB value will be adapted for another important microwave line at 183 GHz. These values have been applied in the MonoRTM radiative transfer model and yielded a good agreement with ground-based radiometric measurements from atmospheric radiation measurement (ARM) sites in Oklahoma and Alaska [40].

Another important point to make here is that, in contradiction to our original point of view, the older data (say, before 1960) are not necessarily worse than newer data. Ref. [37] (1945) for example seems to provide a
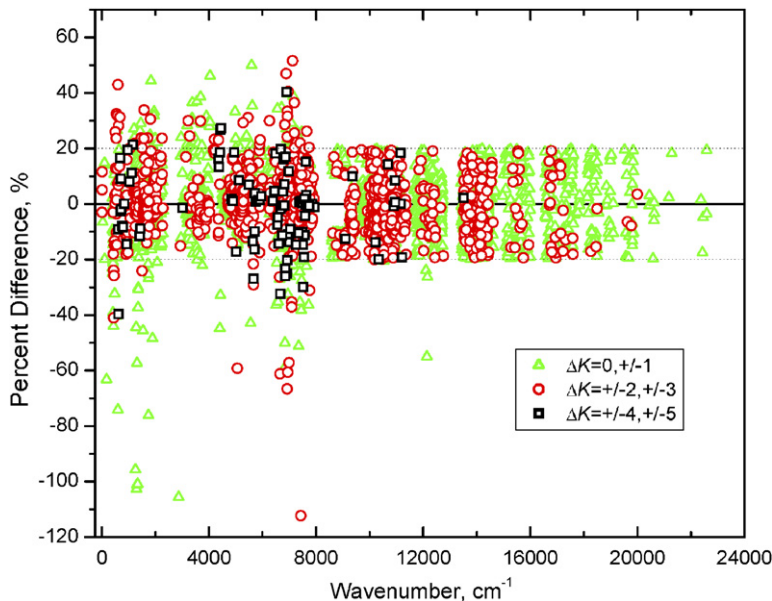

Fig. 5. Percent difference $100 \times (\gamma_{air}(HITRAN2004) - \gamma_{air}(Update))/\gamma_{air}(HITRAN2004)$ plotted against the wavenumber of the corresponding transition.

more accurate value than more recent (1969 and 1970) measurements in Refs. [38,39]. Therefore, it was decided not to remove the data from older references from the GH database as was planned originally.

3. Validation of the new algorithm

The new line list that was created in the course of this work was tested in application to several remote-sensing missions. Below some of these missions are described and results of their validation of our new line list are presented.

3.1. Ground-based measurements: atmospherically emitted radiance interferometer (AERI-ER)

The water vapor ν_2 spectral region is commonly used for passive infrared remote sensing due to its large opacity range. The far-infrared pure rotational water-vapor band is an important spectral region for earth energy budget climate studies. The pure rotational region has a larger contribution to the longwave cooling rates [41], as it is closer to the peak of the blackbody radiance curve at terrestrial atmospheric temperatures. Therefore, it is important that the radiative transfer calculation, especially the spectroscopic parameters and the continuum, be as accurate as possible in the far-infrared region. Due to the limited utilization of the far infrared for remote sensing, there are not a lot of instruments monitoring the atmosphere in the infrared that can be used for validating the radiative transfer calculations in the far-infrared region. The Atmospheric Radiation and Measurement (ARM) program operates a ground-based extended range AERI-ER at the North Slopes of Alaska (NSA) that measures down to $400\,cm^{-1}$ in the infrared. Since the vertical distribution of water vapor in the atmosphere is significantly weighted towards the surface, the ground-based observations in the strong-absorbing pure-rotation band must be performed under conditions of very low atmospheric water-vapor loading in order for the lines not to become opaque close to the instrument. In addition, since the measurements are ground-based, the pressure-broadened widths are important in the line-by-line radiance calculations.

Presented in Fig. 6 is an example of a comparison of the Line-By-Line Radiative Transfer Model (LBLRTM) [42] calculations with AERI-ER observations in the far infrared that demonstrates the impact of recent versions of the water-vapor spectroscopic lines in the *HITRAN* database. The AERI-ER NSA downwelling radiance observations on March 11, 2001 were performed at the surface with a spectral resolution of $0.48\,cm^{-1}$. The temperature and water-vapor profiles used in the LBLRTM calculation were obtained from a radiosonde launched from the NSA ARM site, which was coincident and co-located with the AERI-ER measurements. In order to account for inaccuracies in the radiosonde water-vapor measurements [43], the water-vapor profile was scaled with a retrieved total column water vapor. This case has a very low water-vapor loading of 0.17 perceptible cm, allowing for the observation of stronger water-vapor lines that are typically opaque. Fig. 6 shows that the radiance residuals (AERI-LBLRTM) in this region differ significantly when the calculations use *HITRAN*2004 compared with *HITRAN*2000 plus updates (*HITRAN*2000+) [44]. These residuals indicate that the air-broadened half-widths in the initial release of *HITRAN*2004 were not as accurate as in the previous *HITRAN*2000+. This work was the basis of the re-evaluation and updates made to the initial *HITRAN*2004 water-vapor line parameters outlined in this article. Radiance residuals in Fig. 6 show that the updated *HITRAN*2004 (*HITRAN*2004+) water lines are an improvement over the initial *HITRAN*2004 release and slightly better than the results obtained when using *HITRAN*2000+ water-vapor lines in the LBLRTM calculation. In the first five rows of Table 2, a change of air-broadened half-widths in the *HITRAN* database for several transitions in the range of interest is shown. The frequencies are taken from the *HITRAN*2004 edition. In the *HITRAN*2004 database, some of the γ_{air} were determined by taking an average of the measurements available for the transition. As can be seen in that region, none of the measurements have cleared the filtering procedure and therefore were replaced with CRB calculations, which proved to be quite accurate.

The new line list was also tested against the ground-based Fourier transform spectrometer observations in the $1000–2000\,cm^{-1}$ region acquired during the Italian phase of the EAQUATE campaign [45]. The authors of Ref. [45] have tested the data from *HITRAN*2000, *HITRAN*2004, and the current update and concluded that the latter yields the highest consistency with the observations.
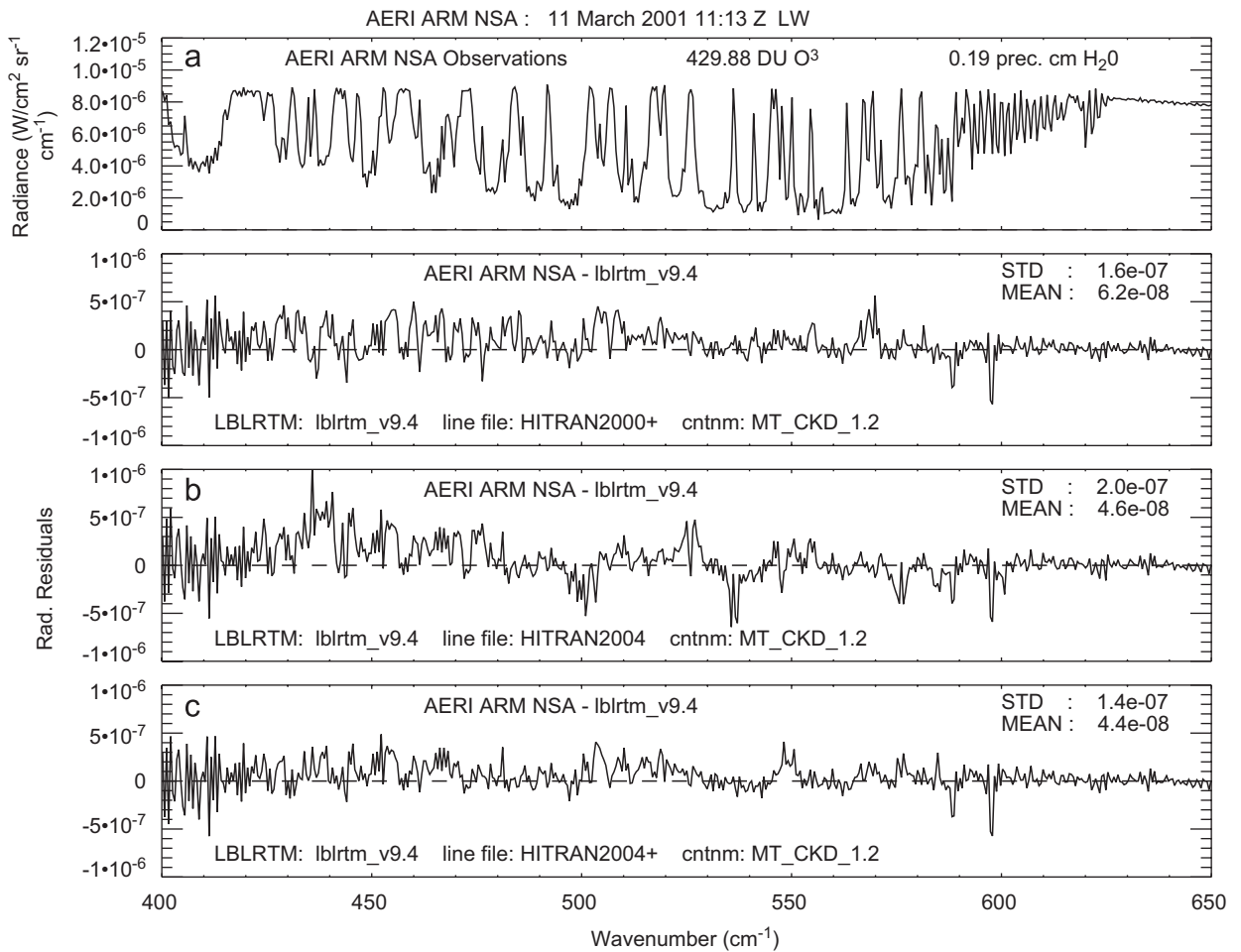
Fig. 6. A comparison example of LBLRTM [42] calculations with AERI-ER observations that demonstrates the impact of recent versions of the water-vapor spectroscopic lines in the *HITRAN* database.

Table 2
Examples of the changes of air-broadened half-widths in the *HITRAN* database

Wavenumber (cm^{-1})	Intensity (cm molecule^{-1})	γ_{air}—2004 (cm^{-1} atm^{-1})	Source in *HITRAN*2004[a]	γ_{air}—Update (cm^{-1} atm^{-1})	Source in update
441.7140	3.645E−21	0.0605	[35]	0.0853	[8]
502.2564	1.733E−20	0.0769	[31,35]	0.0569	[8]
536.2459	1.355E−21	0.1051	[31,34]	0.0802	[8]
576.1144	6.235E−21	0.0631	[31,35]	0.0464	[8]
600.1034	2.382E−21	0.0702	[31]	0.0400	[8]
1987.3401	1.364E−23	0.1008	[4,33]	0.0927	[4]

[a]If more than one source is listed, it means that the average of the values reported in these sources is taken.

3.2. Limb measurements from satellite and balloons

The new air-broadened half-width values were also validated in different missions performing remote sensing above the lower troposphere.

The Atmospheric Chemistry Experiment (ACE), a satellite mission for remote sensing of the Earth's atmosphere developed by the Canadian Space Agency, features a high-resolution infrared Fourier transform spectrometer measuring in occultation mode [46]. In ACE retrievals, only small portions of the spectrum (typically 0.3–$1\,cm^{-1}$) are being analyzed, rather than the entire spectrum. These microwindows are chosen in a way that most of their spectral features belong to the molecule of interest, assuming that known spectroscopic parameters for these features are accurate [47]. For H_2O retrievals from ACE, the new set of broadening parameters yields improved residuals at low altitudes relative to the residuals using *HITRAN*2004 parameters, leading to a decrease in fitting chi-squared of the order of 10%. Considering that the altitudes in these retrievals are above $5\,km$ where the pressure of air is less than that on the ground, and that parameters for the transitions in selected microwindows are considered to have sufficient accuracy already, the 10% improvement is a significant achievement.

In Fig. 7, an example of such improvement is presented, and the decrease in the residual is apparent when the update described in this paper is used. The evolution of the air-broadened half-widths of this line in the *HITRAN* database is presented in the last row of Table 2. In the *HITRAN*2004 edition, the average of available experimental values was used; in the current update only the measurements from Ref. [4] have passed the filtering procedure, yielding a more accurate value for air-broadened half-width.

However, there remain significant w-shaped residuals in the fitting of H_2O lines for ACE spectra, features consistent with line shape effects from changes of velocity during collisions and/or the dependence of collisional parameters on absorber velocity [48]. This suggests that the Voigt function is not sufficiently accurate for H_2O in the ACE spectra, and future processing of the ACE measurements will therefore employ a more complex line-shape function for H_2O, such as the speed-dependent Voigt function [48].

The new update was also used in retrievals of temperature and water-vapor profiles from broad-band measurements of the atmospheric emission spectrum in the 100–$1000\,cm^{-1}$ region acquired by a balloon-borne FT spectrometer (nadir sounding) [49]. The chi-square value of the fit was 0.960, whereas it was 0.988 when using the original *HITRAN*2004 [50]. The improvement may seem to be very slight, but again the pressure of air is low and the effect of the accuracy of values of air-broadened half-widths on the retrievals is lower.

4. Conclusions and potential improvements

When one has to pick the most accurate value out of several originating from different imperfect sources, there are numerous ways of accomplishing this feat. However, one should realize that none of these ways will be absolutely flawless. In this work, an algorithm for choosing values of air-broadened half-widths for inclusion into the *HITRAN* database was developed based on the physical principles and statistics. We do not claim that this algorithm is the best possible solution of the problem. Nevertheless, the new algorithm
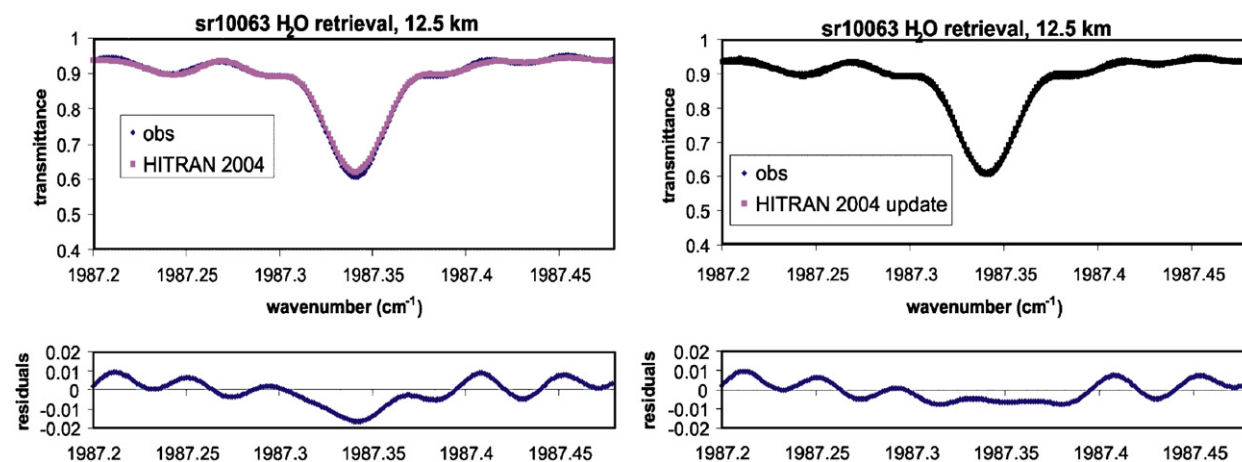

Fig. 7. Comparison of molecular profiles measured with ACE-FTS and the ones calculated using HITRAN2004 and the update described in this paper.

provided significant improvement to the current *HITRAN*2004 edition, as was demonstrated in the validation in application to different remote-sensing missions. This work is an excellent example of fruitful collaboration between the *HITRAN* project and end users, which is extremely important for the continuous improvement of the *HITRAN* database. In total, air-broadened half-width values were updated for 11,787 transitions of water vapor in the *HITRAN*2004 database (6789 for $H_2^{16}O$, 2906 for $H_2^{17}O$, and 2092 for $H_2^{18}O$). A supplementary file listing transitions with changed air-broadened half-widths is provided.

In order to improve the current list further, more experimental works are desirable, especially in the near-IR region. There have already been a number of publications extending data existing in the GH database. The CRB calculations have proven to be a good alternative to the experimental values, especially considering that it is a little easier to anticipate where CRB values will be inaccurate. The CRB values for shorter wavelength regions [17] will be included into the algorithm. Nevertheless, further developments of the CRB method are needed, to be more confident in the theoretical values throughout the entire frequency range. In particular, the intermolecular potential constants will need to be better determined and the use of wavefunctions from *ab initio* calculations will replace the Watson Hamiltonian approach. When a significant bulk of new theoretical and experimental values becomes available, it would also be useful to update existing semi-empirical calculations.

Other pressure-induced parameters of water vapor are needed for some improvements in *HITRAN*. For example, the temperature dependences of air-broadened half-widths will be updated based on the work of Toth et al. [51].

5. Other updates to the water-vapor parameters in *HITRAN*2004

The $H_2^{18}O$ parameters have been updated and $H_2^{17}O$ parameters have been added in the $3v + \delta$ and $4v$ polyad region using data from Tanaka et al. [52].

Twenty-five lines in the $14{,}468$–$14{,}558\,cm^{-1}$ region were removed from the database according to the recommendation by Tolchenov et al. [53] as these lines were in fact due to the oxygen molecule. In the near future, line assignments, intensities and positions for the principal isotopologue of water will be updated in the 9250–$26{,}000\,cm^{-1}$ region using data from Ref. [53].

Acknowledgments

Appendix A. Supplementary Materials

Supplementary data associated with this article can be found in the online version at doi:10.1016/ j.jqsrt.2007.06.009.

References

[1] Rothman LS, Jacquemart D, Barbe A, Benner DC, Birk M, Brown LR, et al. The HITRAN 2004 molecular spectroscopic database. JQSRT 2005;96:139–204.
[2] Chu WP, Chiou EW, Larsen JC, Thomason LW, Rind D, Buglia JJ, et al. Algorithms and sensitivity analyses for stratospheric aerosol and gas experiment-II water-vapor retrieval. J Geophys Res Atm 1993;98:4857–66.
[3] Gamache RR, Hartmann JM. An intercomparison of measured pressure-broadening and pressure-shifting parameters of water vapor. Can J Chem 2004;82:1013–27.
[4] Toth RA. Air- and N_2-broadening parameters of water vapor: 604–2271 cm^{-1}. J Mol Spectrosc 2000;201:218–43.
[5] Toth RA. Measurements and analysis (using empirical functions for widths) of air- and self-broadening parameters of H_2O. JQSRT 2005;94:1–50.
[6] Robert D, Bonamy J. Short range force effects in semiclassical molecular line broadening calculations. J Phys 1979;40:923–43.

[7] Gamache RR, Fisher J. Half-widths of $H_2^{16}O$, $H_2^{18}O$, $H_2^{17}O$, $HD^{16}O$, and $D_2^{16}O$: I. Comparison between isotopomers. JQSRT 2003;78:289–304.

[8] Gamache RR. Line shape parameters of water vapor in the 3.2–17.76 μm region for atmospheric applications. J Mol Spectrosc 2005;229:9–18.

[9] Watson JKG. Determination of centrifugal distortion coefficients of asymmetric-top molecules. J Chem Phys 1967;46:1935–49.

[10] Jacquemart D, Gamache RR, Rothman LS. Semi-empirical calculation of air-broadened half-widths and air pressure-induced frequency shifts of water-vapor absorption lines. JQSRT 2005;96:205–39.

[11] Toth RA. Linelist of water vapor parameters from 500 to 8000 cm^{-1}. ⟨http://mark4sun.jpl.nasa.gov/data/spec/H2O⟩.

[12] Zou Q, Varanasi P. Laboratory measurement of the spectroscopy line parameters of water vapor in the 610–2100 and 3000–4050 cm^{-1} regions at lower-tropospheric temperatures. JQSRT 2003;82:45–98.

[13] Merienne MF, Jenouvrier A, Hermans C, Vandaele AC, Carleer M, Clerbaux C, et al. Water vapor line parameters in the 13000–9250 cm^{-1} region. JQSRT 2003;82:99–117.

[14] Brown LR, Toth RA, Dulick M. Empirical line parameters of $H_2^{16}O$ near 0.94 μm: positions, intensities and air-broadening coefficients. J Mol Spectrosc 2002;212:57–82.

[15] Fally S, Coheur PF, Carleer M, Clerbaux C, Colin R, Jenouvrier A, et al. Water vapor line broadening and shifting by air in the 26000–13000 cm^{-1} region. JQSRT 2003;82:119–31.

[16] Gamache RR, Hartmann JM. Collisional parameters of H_2O lines: effects of vibration. JQSRT 2004;83:119–47.

[17] Gamache RR, Fisher J. Calculated halfwidths and lineshifts of water vapor transitions in the 0.7 μm region and a comparison with published data. J Mol Spectrosc 2001;207:254–62.

[18] Schermaul R, Learner RCM, Newnham DA, Williams RG, Ballard J, Zobov NF, et al. The water vapor spectrum in the region 8600–15000 cm^{-1}: experimental and theoretical studies to a new spectral line database. J Mol Spectrosc 2001;208:32–42.

[19] Massielo G, Esposito F, Grieco G, Pavese G, Restieri R, Serio C, et al. Fitting LBLRTM synthetic spectral radiance to REFIR/BB and BOMEM MR100 down-welling spectra 400 to 1100 cm^{-1}. O-R-9, ASSFTS 2005—12th workshop, Québec City, Canada, May 18–20, 2005.

[20] Shephard MW, Clough SA, Delamere JS, Cady-Pereira K, Mlawer EJ. Validation of the forward model with interferometric measurements for passive remote sensing. O-R-11, ASSFTS 2005—12th Workshop, Québec City, Canada, May 18–20, 2005.

[21] Chang YS, Shaw JH. Intensities and widths of H_2O lines between 1800 and 2100 cm^{-1}. JQSRT 1977;18:491–9.

[22] Malathy Devi V, Benner DC, Rinsland CP, Smith MAH, Sidney BD. Diode laser measurements of air and nitrogen broadening in the v_2 bands of HDO, $H_2^{16}O$, and $H_2^{18}O$. J Mol Spectrosc 1986;117:403–7.

[23] Rinsland CP, Goldman A, Smith MAH, Malathy Devi V. Measurements of Lorentz air-broadening coefficients and relative intensities in the $H_2^{16}O$ pure rotational and v_2 bands from long horizontal path atmospheric spectra. Appl Opt 1991;30:1427–38.

[24] Nicolaisen FM. 1990 ASA workshop paper 5.8, Moscow, June 6–8, 1990.

[25] Cardinet P, Sverin F, Valentin A, Claude ML, Henri A. Wavenumber, intensity and width of water vapour lines in the region of 5.3 μm. C R Acad Sci Paris 1977;284:37–9.

[26] Eng RS, Kelley PL, Mooradian A, Calawa AR, Harman TC. Tunable laser measurements of water vapor transitions in the vicinity of 5 μm. Chem Phys Lett 1973;19:524–8.

[27] Eng RS, Kelley PL, Calawa AR, Harman TC, Nill KW. Tunable diode laser measurements of water vapour absorption line parameters. Molec Phys 1974;28:653–64.

[28] Giesen T, Schieder R, Winnewisser G, Yamada KMT. Precise measurements of pressure broadening and shift for several H_2O lines in the v_2 band by argon, nitrogen, oxygen, and air. J Mol Spectrosc 1992;153:406–18.

[29] Remedios JJ. PhD thesis, University of Oxford, 1990

[30] Mandin JY, Dana V, Badaoui M, Barbe A, Hamdouni A, Plateaux JJ. Measurements of pressure-broadening and pressure-shifting coefficients from FT spectra. J Mol Spectrosc 1994;164:328–37.

[31] Izatt JR, Sakai H, Benedict WS. Positions, intensities, and widths of water-vapor lines between 475 and 692 cm^{-1}. J Opt Soc Am 1969;59:19–26.

[32] Mucha JA. Tunable diode laser measurements of water vapor line parameters in the 6-μm spectral region. Appl Spectrosc 1982;36:141–7.

[33] Yamada KMT, Harter M, Giesen T. Survey study of air-broadened water vapor lines in the v_2 band by high-resolution FTIR spectroscopy. J Mol Spectrosc 1993;157:84–94.

[34] Adel A. Absorption line width in the rotation spectrum of atmospheric water vapor. Phys Rev 1947;71:806–8.

[35] Steyert DW, Wang WF, Sirota JM, Donahue NM, Reuter DC. Pressure broadening coefficients for rotational transitions of water in the 380–600 cm^{-1} range. JQSRT 2002;72:775–82.

[36] Lucchesini A, Gozzini S, Gabbanini C. Water vapor overtones pressure line broadening and shifting measurements. Eur Phys J D 2000;8:223–6.

[37] Becker GE, Autler SH. Water vapor absorption of electromagnetic radiation in the centimeter wave-length range. Phys Rev 1946;70:300–7.

[38] Liebe HJ, Dillon TA. Accurate foreign-gas-broadening parameters of the 22-GHz H_2O line from refraction spectroscopy. J Chem Phys 1969;50:727–32.

[39] Mrowinski D. Refraction and absorption in atmospheric gases near the 22 GHz water vapour rotational line. Z Angew Phys 1970;29:323–30.

[40] Payne VH, Delamere JS, Cady-Pereira KE, Gamache RR, Moncet J-L, Mlawer E, et al. Air-broadened half-widths of the 22 GHz and 183 GHz water vapor lines. IEEE Trans Geosci Remote Sens 2007, submitted for publication.

[41] Clough SA, Iacono MJ, Moncet JL. Line-by-line calculations of atmospheric fluxes and cooling rates: application to water vapor. J Geophys Res 1992;97:15761–85.

[42] Clough SA, Shephard MW, Mlawer EJ, Delamere JS, Iacono MJ, Cady-Pereira K, et al. Atmospheric radiative transfer modeling: a summary of AER codes. JQSRT 2005;91:233–4.

[43] Turner DD, Lesht BH, Clough SA, Liljegren JC, Revercomb HE, Tobin DC. Dry bias and variability in Vaisala RS80-H radiosondes: the ARM experience. J Atmos Ocean Technol 2004;20:117–32.

[44] Rothman LS, Barbe A, Benner DC, Brown LR, Camy-Peyret C, Carleer MR, et al. The HITRAN molecular spectroscopic database: edition of 2000 including updates through 2001. JQSRT 2003;82:5–44.

[45] Taylor JP, Smith WL, Cuomo V, Larar AM, Zhou DK, Serio C, et al. EAQUATE: an international experiment for hyper-spectral atmospheric sounding validation. Bull Am Meteorol Soc 2007, in press.
Esposito F, Grieco G, Masiello G, Pavese G, Restieri R, Serio C, et al. Intercomparison among line-parameters spectroscopic databases using downwelling spectral radiance. Q J R Meteorol Soc, 2007, in press.

[46] Bernath PF, McElroy CT, Abrams MC, Boone CD, Butler M, Camy-Peyret C, et al. Atmospheric chemistry experiment (ACE): mission overview. Geophys Res Lett 2005;32:L15S01.

[47] Boone CD, Nassar R, Walker KA, Rochon YJ, McLeod SD, Rinsland CP, et al. Retrievals for the atmospheric chemistry experiment Fourier-transform spectrometer. Appl Opt 2005;44:7218–30.

[48] Boone CD, Walker KA, Bernath PF. Speed-dependent Voigt profile for water vapor in infrared remote sensing applications. JQSRT 2007;105:525–32.

[49] Bianchini G, Palchetti L, Belotti C, Del Bianco S, Cortesi U. Wide-band spectrally resolved measurement of the Earth's up-welling radiation with the REFIR-PAD spectroradiometer. Remote Sensing of Clouds and the Atmosphere XI, 6362. SPIE; 2006. p. 63622K-1–9.

[50] Cortesi U. Private communication, 2006.

[51] Toth RA, Brown LR, Smith MAH, Malathy Devi V, Benner DC, Dulick M. Air-broadening of H_2O as a function of temperature: 696–2163 cm^{-1}. JQSRT 2006;101:339–66.

[52] Tanaka M, Naumenko O, Brault J, Tennyson J. Fourier transform absorption spectra of $H_2^{18}O$ and $H_2^{17}O$ in the $3v + \delta$ and $4v$ polyad region. J Mol Spectrosc 2005;234:1–9.

[53] Tolchenov RN, Naumenko O, Zobov NF, Shirin SV, Polyansky OL, Tennyson J, et al. Water vapour line assignments in the 9250–26000 cm^{-1} frequency range. J Mol Spectrosc 2005;233:68–76.